Phosphorescence Enhancement Triggered by Π Stacking in Solid-State [Cu(N−N)(P−P)]BF_4 Complexes

Liming Zhang,[†,‡] Bin Li,*[,†] and Zhongmin Su[§]

Key Laboratory of Excited State Processes, Changchun Institute of Optics, Fine Mechanics and Physics, Chinese Academy of Sciences, Changchun 130033, PR China, Graduate School of the Chinese Academy of Sciences, Chinese Academy of Sciences, Beijing 100039, PR China, and Department of Chemistry, Northeast Normal University, Changchun 130024, PR China

Received November 18, 2008. Revised Manuscript Received December 24, 2008

In this article, we report a phosphorescence enhancement phenomenon of [Cu(N−N)(P−P)]BF_4 complexes in the solid state. The phosphorescence enhancement phenomenon is composed of three features: (1) an obvious emission blue shift, (2) a greatly enhanced photoluminescence quantum yield, and (3) a longer excited-state lifetime. Systematic analyses prove that the main cause of this phenomenon is nonradiative process suppression triggered by the π stacking between [Cu(N−N)(P−P)]BF_4 molecules. The phorsphorescence enhancement widely exists in [Cu(N−N)(P−P)]BF_4 complexes because of the π surfaces in their diimine ligands.

Introduction

The development of practical components for chemical sensors, display devices, probes of biological systems, and solar energy conversion schemes has sparked an interest in complexes of diimine ligands with transition metals, especially heavy metal ions such as ruthenium(II) and rhenium(I).[1−9] At the same time, the strong appeal of using cheaper copper(I) complexes to replace more expensive compounds based on ruthenium(II) or other metal ions and the need for a deeper understanding of correlation between structural processes and photophysical properties have led to continuous progress in the design of photoluminescent Cu(I) complexes. However, the emission signal from the charge-transfer (CT) excited state of copper(I) complexes is typically weak and short-lived because the lowest-energy CT state of a d^{10} system involves excitation from a metal−ligand dσ* orbital.[10−12] An important consequence is that the excited state typically prefers tetragonally flattened geometry, whereas the ground state usually adopts a more tetrahedral-like coordination geometry that is appropriate for a closed-shell ion.[10,13] Aside from reducing the energy content, the geometry relaxation that occurs in the excited state facilitates relaxation back to the ground state.[14,15] Moreover, donor media also tend to quench the excited state. Blaskie and McMillin first reported this type of exciplex quenching, and by now, many other studies have confirmed the mechanism. Mixed-ligand systems involving triphenylphosphane looked promising because they exhibited long excited-state lifetimes in the solid state and in frozen solution.[16−19] A series of new mixed-ligand copper(I) polypyridine and phenanthroline complexes such as $[Cu(N−N)(POP)]^+$ [POP = bis(2-(diphenylphosphanyl)phenyl) ether], which are superior emitters, have been synthesized. It is found that solvent-induced exciplex quenching is relatively inefficient for the CT excited state of this POP system. However, the introduction of sterically blocking ligands can impede geometric relaxation as well as solvent attack. Here, steric effects cooperate effectively to block the excited state close to the ground-state geometry. The metal-to-ligand charge-transfer (MLCT) excited states of cuprous diimine compounds are often luminescent and play important roles in photoinduced electron and energy transfer. McCormick and Wang also reported that both steric and electronic properties of phosphorus ancillary ligands have impacts on the electrochemical properties of the copper complexes.[20−22]

The theoretical studies reported by Sakaki and Feng on the $[Cu(N−N)(P−P)]^+$ system prove that the tetrahedral-like coordination geometry is more stable than the tetragonally flattened geometry by 16.5 kcal/mol in the $^1A_1$ ground state, whereas

* Corresponding author. Tel/Fax: +86431 86176935. E-mail address: lib020@ciomp.ac.cn.

† Changchun Institute of Optics, Fine Mechanics and Physics, Chinese Academy of Sciences.

‡ Graduate School of the Chinese Academy of Sciences, Chinese Academy of Sciences.

§ Northeast Normal University.

(1) De Silva, P.; Fox, D. B.; Moody, T. S.; Weir, S. M. *Pure Appl. Chem.* **2001**, *73*, 503.
(2) Rudzinski, M.; Nocera, D. G. *Mol. Supramol. Photochem.* **2001**, *7*, 1.
(3) Elliott, M.; Pichot, F.; Bloom, C. J.; Rider, L. S. *J. Am. Chem. Soc.* **1998**, *120*, 6781.
(4) Zhao, Y. D.; Richman, A.; Storey, C.; Radford, N. B.; Pantano, P. *Anal. Chem.* **1999**, *71*, 3887.
(5) Erkkila, K. E.; Odom, D. T.; Barton, J. K. *Chem. Rev.* **1999**, *99*, 2777.
(6) Prodi, L.; Bolletta, F.; Montaltri, M.; Zaccheroni, N. *Coord. Chem. Rev.* **2000**, *205*, 59.
(7) Balzani, V.; Juris, A.; Venturi, M.; Campagna, S.; Serroni, S. *Chem. Rev.* **1996**, *96*, 759.
(8) El-Safty, S. A.; Prabhakaran, D.; Ismail, A. A.; Matsunaga, H.; Mizukami, F. *Adv. Funct. Mater.* **2007**, *17*, 3731.
(9) El-Safty, S. A.; Ismail, A. A.; Matsunaga, H.; Mizukami, F. *Chem. Eur. J.* **2007**, *13*, 9245.
(10) McMillin, D. R.; McNett, K. M. *Chem. Rev.* **1998**, *98*, 1201.
(11) Armaroli, N. *Chem. Soc. Rev.* **2001**, *30*, 113.
(12) Scaltrito, D. V.; Thompson, D. W.; O'Callaghan, J. A.; Meyer, G. J. *Coord. Chem. Rev.* **2000**, *208*, 243.
(13) Zhang, Q.; Zhou, Q.; Cheng, Y.; Wang, L.; Ma, D.; Jing, X.; Wang, F. *Adv. Mater.* **2004**, *16*, 432.
(14) Eggleston, K.; McMillin, D. R.; Koenig, K. S.; Pallenberg, A. J. *Inorg. Chem.* **1997**, *36*, 172.
(15) Cunningham, T.; Cunningham, K. L. H.; Michalec, J. F.; McMillin, D. R. *Inorg. Chem.* **1999**, *38*, 4388.
(16) Rader, R. A.; McMillin, D.; Buckner, M. T.; Matthews, T. G.; Casadonte, D. J.; Lengel, R. K.; Whittaker, S. B.; Darmon, L. M.; Lytle, F. E. *J. Am. Chem. Soc.* **1981**, *103*, 5906.
(17) Breddels, P. A.; Berdowski, M.; Blasse, G. *J. Chem. Soc. Faraday Trans. 2* **1982**, *78*, 595.
(18) Palmer, E. A.; McMillin, D. R. *Inorg. Chem.* **1987**, *26*, 3837.
(19) Kranenburg, M.; Van der Burgt, Y. E. M.; Kamer, P. C. J.; Van Leeuwen, P. W. N. M.; Goubitz, K.; Fraanje, J. *Organometallics* **1995**, *14*, 3081.
(20) McCormick, T.; Jia, W. L.; Wang, S. *Inorg. Chem.* **2006**, *45*, 147.
(21) Cuttell, D. G.; Kuang, S. M.; Fanwick, P. E.; McMillin, D. R.; Walton, R. A. *J. Am. Chem. Soc.* **2002**, *124*, 6.
(22) Kuang, S. M.; Cuttel, D. G.; McMillin, D. R.; Fanwick, P. E.; Walton, R. A. *Inorg. Chem.* **2002**, *41*, 3313.

10.1021/la803822s CCC: $40.75
Published on Web 01/26/2009

Scheme 1. Molecular Structures of the Compounds

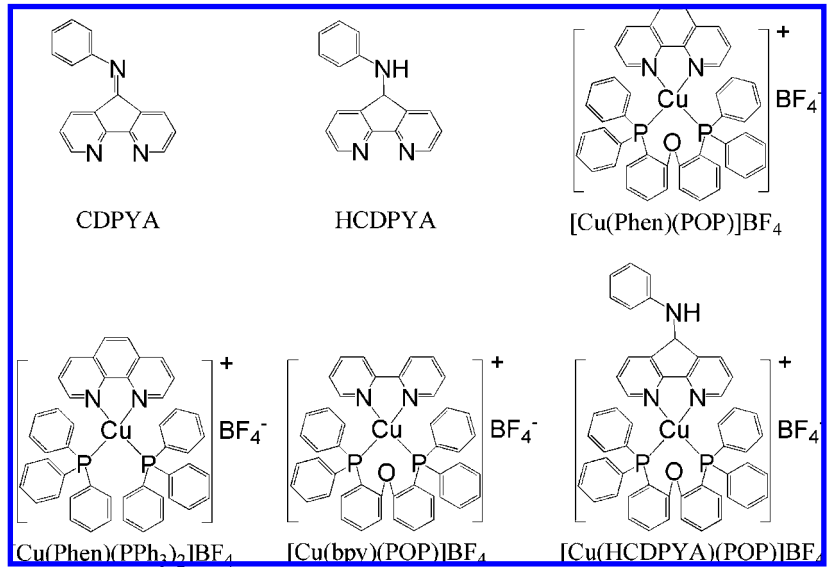

tetragonally flattened geometry is more stable than tetrahedral-like coordination geometry by 4.1 kcal/mol in the $^3A_2$ MLCT excited state.[23] For a typical phosphorescent Cu(I) complex, the two highest occupied molecular orbitals (HOMOs) have predominant metal Cu d character, admixed with some contributions from the phosphorus ligand, whereas the two lowest unoccupied orbitals (LUMOs) are essentially π^* orbitals localized on the diimine ligand. The photoluminescence corresponds to the lowest triplet T_1 and is thus assigned as a characteristic of MLCT [d(Cu) $\rightarrow \pi^*$(diimine ligand)].[24] McCormick and Wang also confirmed that HOMO is dominated by the d orbital of the copper(I) ion, mixed with contributions from the phosphorus ligands and a small contribution from the diimine ligand.[20]

In contrast to the systematically experimental and theoretical studies on the electronic and photophysical properties of the $[Cu(N-N)(P-P)]^+$ system, little effort has been devoted to weak interactions between molecules that greatly influence the photophysical properties.[25−30] In the reports of Thummel and coworks, it is found that $[Cu(L)_2]^+$ (L, based on 2-(2′-pyridyl)-benzo[*h*]quinoline and 2,2′-bibenzo[*h*]quinoline) complexes profit from stabilization associated with π-stacking interactions by exhibiting a long excited-state lifetime of 5.3 μs and a quantum yield of 0.10.[25]

In this article, we report a commonly existing phosphorescence enhancement phenomenon of $[Cu(N-N)(P-P)]BF_4$ complexes in the solid state. Systematic studies suggest that the main cause of this phenomenon is nonradiative process suppression triggered by the π-stacking between $[Cu(N-N)(P-P)]BF_4$ molecules.

Experimental Method

Compounds studied in this article are shown in Scheme 1. Bis(2-(diphenylphosphanyl)phenyl) ether (POP), PPh_3, 1,10-phenanthroline (phen), 2,2′-bipyridine (bpy), and $Cu(BF_4)_2$ were purchased from Aldrich Chemical Co. and used without further purification.

Synthesis of Compounds. *Cyclopenta[2,1-b;3,4-b′]dipyridin-5-ylidene-phenyl-amine (CDYPA).* CDYPA was synthesized according to a literature procedure.[31] ^{1}H NMR ($CDCl_3$): δ 8.81 (s, 1 H), 8.65 (s, 1 H), 8.25 (s, 1 H), 7.46−7.40 (m, 3 H), 7.28−7.18 (m, 2 H), 7.01−6.98 (m, 3 H). Anal. Calcd for $C_{17}H_{11}N_3$: C, 79.36; H, 4.31; N, 16.33. Found: C, 79.18; H, 4.50; N, 16.21.

(5H-Cyclopenta[2,1-b;3,4-b′]dipyridin-5-yl)-phenylamine (HCDYPA). HCDYPA was synthesized by adding excess $NaBH_4$ to a solution of CDYPA in MeOH and was stirred for 4 h under N_2, and then the crude product was purified by recrystallization in EtOH. ^{1}H NMR ($CDCl_3$): δ 8.75 (s, 2 H), 7.93 (s, 2 H), 7.24−7.18 (s, 3 H), 6.86−6.84 (m, 3 H), 5.75 (s, 1H), 4.05 (s, 1H), 1.85 (s, 1H). Anal. Calcd for $C_{17}H_{13}N_3$: C, 78.74; H, 5.05; N, 16.20. Found: C, 78.65; H, 5.11; N, 16.11.

[Cu(phen)(POP)]BF_4, [Cu(phen)(PPh_3)$_2$]BF_4, and [Cu(bpy)(POP)]BF_4. These were synthesized according to the literature procedures.[13,24] The standard samples are denoted as S-[Cu(phen)(POP)]BF_4, S-[Cu(phen)(PPh_3)$_2$]BF_4, and S-[Cu(bpy)(POP)]BF_4, respectively.

S-[Cu(phen)(POP)]BF_4. Anal. Calcd for $C_{48}H_{36}BCuF_4N_2OP_2$: C, 66.33; H, 4.18; N, 3.22. Found: C, 66.21; H, 4.31; N, 3.28.

S-[Cu(phen)(PPh_3)$_2$]BF_4. Anal. Calcd for $C_{48}H_{38}BCuF_4N_2P_2$: C, 67.42; H, 4.48; N, 3.28. Found: C, 67.27; H, 4.60; N, 3.21.

S-[Cu(bpy)(POP)]BF_4. Anal. Calcd for $C_{46}H_{36}BCuF_4N_2OP_2$: C, 65.38; H, 4.29; N, 3.31. Found: C, 65.47; H, 4.41; N, 3.14.

[Cu(HCDPYA)(POP)]BF_4. This compound was synthesized similarly with S-[Cu(phen)(POP)]BF_4. ^{1}H NMR ($CDCl_3$): δ 8.56 (s, 2 H), 7.81 (s, 2 H), 7.37 −6.63 (m, 35 H), 4.05 (s, 1H), 1.85 (s, 1H). ^{31}P NMR: δ + 1.67 (s, $P(C_6H_5)_2C_6H_4$). Anal. Calcd for $C_{53}H_{41}BCuF_4N_3OP_2$: C, 67.13; H, 4.36; N, 4.43. Found: C, 67.27; H, 4.60; N, 4.28.

Phosphorescence-Enhanced [Cu(phen)(POP)]BF_4. This compound was processed as follows and denoted as PE-[Cu(phen)-(POP)]BF_4 via methods A and B.

Method A: 0.5 mmol of S-[Cu(phen)(POP)]BF_4 was dissolved in 5 mL of CH_2Cl_2 at 0 °C. After the addition of ice-cooled *n*-hexane under vigorous stirring, the mixture was then brought to 30 °C for 1 h, filtered, and dried in vacuum at 30 °C. Anal. Calcd and Found: C, 66.25; H, 4.28; N, 3.24.

Method B: 0.5 mmol of S-[Cu(phen)(POP)]BF_4 was dissolved in 5 mL of CH_2Cl_2 at 30 °C. After the addition of *n*-hexane under vigorous stirring, the mixture was stirred at 30 °C for 30 min and then filtered and dried in vacuum at 30 °C. Anal. Calcd and Found: C, 66.19; H, 4.34; N, 3.25.

(23) Sakaki, S.; Mizutani, H.; Kase, Y. I. *Inorg. Chem.* **1992**, *31*, 4575.
(24) Yang, L.; Feng, J. K.; Ren, A. M.; Zhang, M.; Ma, Y. G.; Liu, X. D. *Eur. J. Inorg. Chem.* **2005**, *10*, 1867.
(25) Riesgo, E. C.; Hu, Y. Z.; Bouvier, F.; Thummel, R. P.; Scaltrito, D. V.; Meyer, G. J. *Inorg. Chem.* **2001**, *40*, 3413.
(26) Thomas, K. J.; Sunoj, R. B.; Chandrasekhar, J.; Ramamurthy, V. *Langmuir* **2000**, *16*, 4912.
(27) Nosenko, Y.; Kunitski, M.; Riehn, C.; Thummel, R. P.; Kyrychenko, A.; Herbich, J.; Waluk, J.; Brutschy, B. *J. Phys. Chem. A* **2008**, *112*, 1150.
(28) Herbich, J.; Kijak, M.; Zieliska, A.; Thummel, R. P.; Waluk, J. *J. Phys. Chem. A* **2002**, *106*, 2158.
(29) Petkova, I.; Mudadu, M. S.; Singh, A.; Thummel, R. P.; Stokkum, I. H. M. van.; Buma, W. J.; Waluk, J. *J. Phys. Chem. A* **2007**, *111*, 11400.
(30) Vieira Ferreira, L. F.; Lemos, M. J.; Reis, M. J.; Botelho do Rego, A. M. *Langmuir* **2000**, *16*, 5673.
(31) Tai, Z.; Zhang, G.; Qian, X.; Xiao, S.; Lu, Z.; Wei, Y. *Langmuir* **1993**, *9*, 1601.

Phosphorescence-Enhanced [Cu(phen)(PPh$_3$)$_2$]BF$_4$, [Cu(bpy)(POP)]BF$_4$, and [Cu(HCDPYA)(POP)]BF$_4$. These compounds were similarly processed using method B. They are denoted as PE-[Cu(phen)(PPh$_3$)$_2$]BF$_4$, PE-[Cu(bpy)(POP)]BF$_4$, and PE-[Cu(HCDPYA)(POP)]BF$_4$, respectively.

Measurements. Luminescence lifetimes were obtained with 355 nm light generated from a pumped third-harmonic generator, which uses a pulsed Nd:YAG laser as the excitation source. The Nd:YAG laser possesses a line width of 1.0 cm^{-1}, a pulse duration of 10 ns, and a repetition frequency of 10 Hz. A rhodamine 6G dye pumped by the same Nd:YAG laser was used as the frequency-selective excitation source. All of the photoluminescence (PL) spectra were measured with a Hitachi F-4500 fluorescence spectrophotometer. Solid-state UV−vis absorption spectra were recorded with the Hitachi F-4500 fluorescence spectrophotometer using diffuse reflection scan mode. UV−vis absorption spectra were recorded using a Shimadzu UV-3101PC spectrophotometer. ^{1}H and ^{31}P spectra were obtained with the use of a Varian INOVA 300 spectrometer. Elemental analyses were performed on a Carlo Erba 1106 elemental analyzer. Thermogravimetric analysis was performed on a WRT-2P thermal gravity analyzer. The X-ray diffraction (XRD) patterns were obtained on a Rigaku D/Max-Ra X-ray diffractomemter using a Cu target radiation source (λ = 1.5418 Å). All measurements were carried out in air at room temperature without being specified.

The dipole moment of the [Cu(phen)(POP)]$^+$ moiety was calculated by PC GAMESS using RB3LYP/SBKJC. The initial structure was obtained from single-crystal XRD data.[22]

Results and Discussion

The molecular structure of [Cu(phen)(POP)]BF$_4$ has been identified by single-crystal XRD, and its photophysical properties have been reported and well studied.[13,22] Thus, we choose [Cu(phen)(POP)]BF$_4$ as the discussion model. PE-[Cu(phen)(POP)]BF$_4$ exhibits an obvious emission blue shift under UV (~365 nm) excitation compared with the emission of S-[Cu(phen)(POP)]BF$_4$, making the transformation from S-[Cu(phen)(POP)]BF$_4$ to PE-[Cu(phen)(POP)]BF$_4$ easy to monitor with the naked eye.

Transformation Cycle of [Cu(phen)(POP)]BF$_4$. Figure 1 depicts the transformation cycle from S-[Cu(phen)(POP)]BF$_4$ to PE-[Cu(phen)(POP)]BF$_4$ and then back to S-[Cu(phen)(POP)]BF$_4$. It can be observed that the transformation between S-[Cu(phen)(POP)]BF$_4$ and PE-[Cu(phen)(POP)]BF$_4$ is fully repeatable. samples 1 and 5 are selected to be the discussion models. First, XRD patterns are performed on both samples. The results (Supporting Information) confirm that both samples are in an amorphous state, which eliminates the possibility of the condensed state difference causing photophysical variations.

Stability of [Cu(phen)(POP)]BF$_4$. Elemental analyses suggest that standard [Cu(phen)(POP)]BF$_4$, [Cu(phen)(POP)]BF$_4$ processed with method A, and [Cu(phen)(POP)]BF$_4$ processed with method B all have quite similar C, H, and N components, which indicates that no moiety is lost during the transformation cycle of [Cu(phen)(POP)]BF$_4$. An obvious possibility is that [Cu(phen)(POP)]BF$_4$ retains its molecular structure during the whole process, but there is another possibility. McMillin and co-workers found that some Cu(I) complexes, such as [Cu(dmp)(PPh$_3$)$_2$]BF$_4$ and [Cu(dmp)(POP)]BF$_4$ (dmp = 2,9-dimethyl-1,10-phenanthroline), undergo solvent-dependent ligand redistribution reactions, as shown in eq 1.[22]

$$2[\mathrm{Cu(dmp)(POP)}]^+ = [\mathrm{Cu(dmp)_2}]^+ + [\mathrm{Cu(POP)}]^+ + \mathrm{POP} \quad (1)$$

Obviously, the potential ligand redistribution reaction of [Cu(phen)(POP)]BF$_4$may also fit the elemental analyses. Fortunately, [Cu(phen)(POP)]BF$_4$ does not suffer the solvent-dependent ligand redistribution reaction, and CH_2Cl_2 can efficiently suppress the potential ligand dissociation.[22] It is reported that the decomposition temperature of [Cu(phen)(POP)]BF$_4$ is as high as 593 K.[13] The energy content (E_T) of [Cu(phen)(POP)]BF$_4$ at temperature T can be expressed by eq 2 according to the Dulong−Petit law:

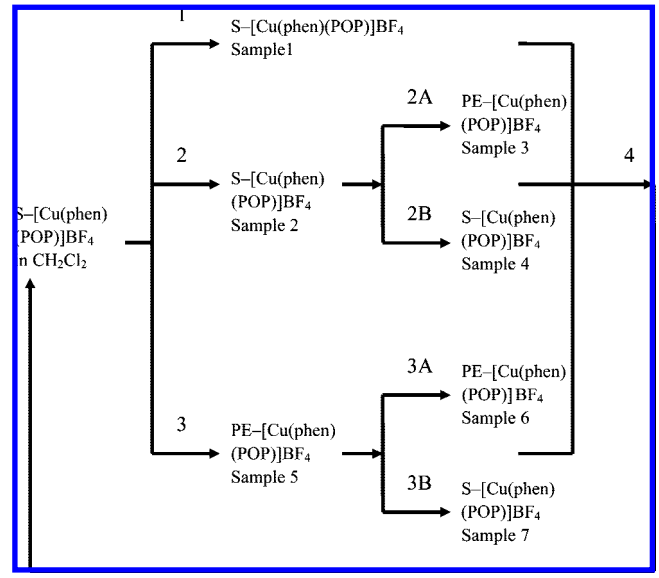

Figure 1. Transformation cycle of [Cu(phen)(POP)]BF$_4$. Conditions: (1) evaporation of the solvent; (2) at 0 °C, the addition of excess *n*-hexane; (2A) stirred at 30 °C for 1 h and then filtered and dried; (2B) stirred at 0 °C for 1 h and then filtered and dried at low temperature; (3) at 30 °C, addition of excess *n*-hexane, stirred for 30 min, and then filtered and dried; (3A) below 30 °C, exposed to air for 4 weeks; (3B) at 60 °C for 30 min and exposed to air; and (4) dissolved in CH_2Cl_2.

$$E_T = 3NkT \quad (2)$$

N denotes the number of particles; here we consult one [Cu(phen)(POP)]BF$_4$ molecule, so N = 123. k denotes the Boltzmann constant, and T denotes the temperature. At 30 °C (303 K), the number of [Cu(phen)(POP)]BF$_4$ molecules owing to the decomposing energy content, N_{decm}, can be expressed according to the Boltzmann distribution law by eq 3

$$N_{\mathrm{decm}} = N_{\mathrm{sum}} \exp(-(E_{593} - E_{303})/kT) \quad (3)$$

N_{sum} is the total number of [Cu(phen)(POP)]BF$_4$ molecules; E_{593} is the energy content of the [Cu(phen)(POP)]BF$_4$ molecule at 593 K; E_{303} is the corresponding value at 303 K; and T denotes the temperature, which is 303 K.

According to eqs 2 and 3, N_{decm} is calculated to be $N_{\mathrm{sum}}e^{-353.17}$, which is small enough to be neglected. Thus, we come to the conclusion that the possibility of [Cu(phen)(POP)]BF$_4$ dissociation can be eliminated in both the solid state and liquid state because its molecular structure is stable enough to experience the transformation cycle.

UV−Vis Absorption Spectra of S-[Cu(phen)(POP)]BF$_4$ and PE-[Cu(phen)(POP)]BF$_4$. UV−vis absorption spectra of the five samples prepared under conditions 1, 2A, 2B, 3A, and 3B in CH_2Cl_2 with a concentration of 1 × 10^{-5} mol/L are shown in Figure 2, and the normalized UV−vis absorption spectra of samples 1 and 5 are given as the inset of Figure 2. It can be observed that their molecular electronic absorptions are exactly the same: the absorption spectrum is composed of a high-energy absorption band ranging from 200 to 350 nm that corresponds to $\pi \rightarrow \pi^*$ transitions of ligands and a low-energy absorption band ranging from 350 to 450 nm that is attributed to MLCT transitions as previously reported.[22,24] Solid-state UV−vis

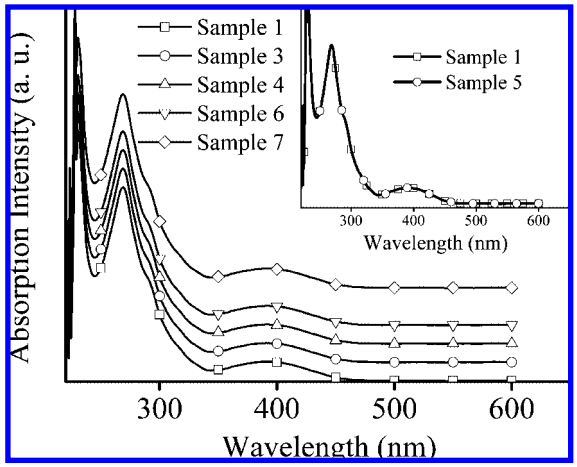

Figure 2. UV−vis absorption of samples in CH_2Cl_2 with a concentration of 1×10^{-5} mol/L. (Inset) Normalized absorption spectra of samples 1 and 5 in CH_2Cl_2 with a concentration of 1×10^{-5} mol/L.

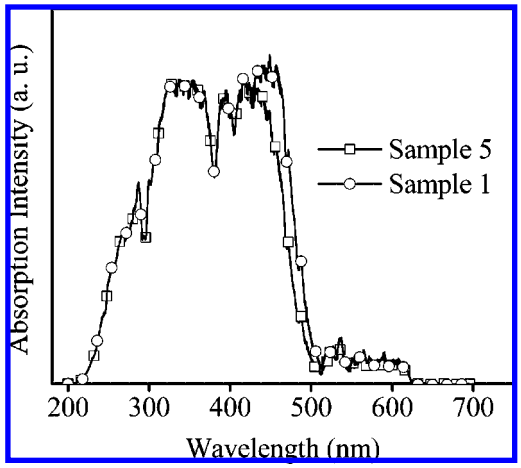

Figure 3. Solid-state UV−vis absorption spectra of samples 1 and 5.

absorption spectra of samples 1 and 5 shown in Figure 3 suggest that there exists a small difference between samples 1 and 5: sample 1 exhibits stronger absorption in the 430−510 nm region than does sample 5. The absorption band in the 200−400 nm region is attributed to intramolecular $\pi \rightarrow \pi^*$ transitions of ligands, which are usually immune to environmental influences. However, the absorption band in the 430−510 nm region is believed to be due to the MLCT transitions, which are usually influenced by factors such as solvents and dipole moments. However, the band shapes of samples 1 and 5 in the 430−510 nm region are quite similar, indicating that the nature of the electronic structure of the transitions is not changed. The decreased absorbance of sample 5 may be caused by the somehow decreased oscillator strengths of the transitions, which will be discussed later, and this decreased absorbance exists only in the solid state.

Thermal Effect on S-[Cu(phen)(POP)]BF_4 and PE-[Cu(phen)-(POP)]BF_4. Figure 1 shows us that low temperature (0 °C) can suppress the transformation from S-[Cu(phen)(POP)]BF_4 to PE-[Cu(phen)(POP)]BF_4 whereas high temperature (60 °C) can transform PE-[Cu(phen)(POP)]BF_4 back to S-[Cu(phen)-(POP)]BF_4. Both S-[Cu(phen)(POP)]BF_4 and PE-[Cu(phen)-(POP)]BF_4 are stable enough at room temperature in air. Thus, it can be concluded that PE-[Cu(phen)(POP)]BF_4 is in a metastable state; the transformation from S-[Cu(phen)(POP)]BF_4 to PE-[Cu(phen)(POP)]BF_4 is an endothermic process, and the inverse

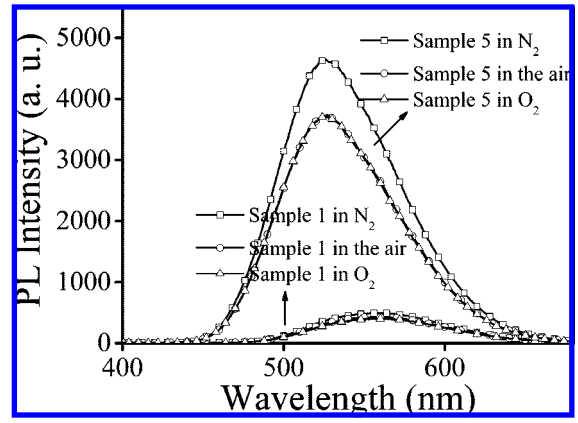

Figure 4. PL of samples 1 and 5 with $\lambda_{ex} = 350$ nm in the solid state.

process needs activation energy to break up the metastable state. Considering that thermal vibration at 60 °C can supply the activation energy, which is calculated to be as small as ∼8.3 kJ/mol by eq 2 (here the amount of PE-[Cu(phen)(POP)]BF_4 is assumed to be 1 mol and thus $N = 6.02 \times 10^{23}$), it is inferred that no new chemical bond is formed and the weak interactions between [Cu(phen)(POP)]BF_4 molecules should be responsible for the formation of the metastable state.

Considering that (1) the [Cu(phen)(POP)]BF_4 molecule is stable enough during the whole transformation cycle; (2) S-[Cu(phen)-(POP)]BF_4 and PE-[Cu(phen)(POP)]BF_4 have the same molecular electronic nature; and (3) the formation of the metastable state of PE-[Cu(phen)(POP)]BF_4 is caused by the weak interactions between [Cu(phen)(POP)]BF_4 molecules, we can say that S-[Cu(phen)(POP)]BF_4 and PE-[Cu(phen)(POP)]BF_4 have the same molecular structure and photophysical differences between S-[Cu(phen)(POP)]BF_4 and PE-[Cu(phen)(POP)]BF_4 may be caused by intermolecular rearrangement in the solid state.

Photophysical Property Analyses of PE-[Cu(phen)(POP)]BF_4. *Variations of the Photophysical Property.* Figure 4 depicts the photoluminescence (PL) of samples 1 and 5 with $\lambda_{ex} = 350$ nm in the solid state. Samples 1 and 5 exhibit broad emission spectra peaking at 560 and 527 nm, respectively, without giving any vibronic progressions, which suggests that the emissive excited states have CT character. Except for the large-scale emission blue shift of sample 5 compared with the emission of sample 1, the emission yield (Φ) of sample 5 is dramatically larger than that of sample 1. Φ of sample 5 is determined to be 0.96 with the method reported by Wang et al.,[13] using sample 1 as a reference ($\Phi = 0.16$). From the emission intensity (I) decay analyses of the two samples, I is found to be expressed by a sum of the two exponential time functions

$$I = A_f \exp(-t/\tau_f) + A_s \exp(-t/\tau_s) \quad \tau_s > \tau_f \qquad (4)$$

where τ_f and A_f are the lifetime and pre-exponential factor for the faster decay, respectively, and τ_s and A_s are those for the slower decay. Lifetimes τ_f and τ_s in the solid state are calculated to be 2.9 and 5.8 μs for sample 1 and 1.4 and 10.0 μs for sample 5. The longer lifetime of sample 5 is confirmed by its greater sensitivity to O_2 ($(I_{N_2})/(I_{O_2}) = 1.25$) than that of sample 1 ($(I_{N_2})/(I_{O_2}) = 1.22$) as shown in Figure 4.

As Feng reported, the photoluminescence of a typical $[Cu(N-N)(P-P)]^+$ corresponds to the lowest triplet T_1, which consists of a transition from HOMO to LUMO or LUMO + 1, and is thus assigned as having a character of MLCT [d(Cu) → π^*(diimine ligand)].[24] In addition, the PL spectral band shape

of sample 1 is unchanged under N_2, air, and O_2 atmospheres except for the decreased emission intensity; a similar case is also observed for sample 5, as shown in Figure 4. Thus, the faster and slower decay components are considered to have the same electronic nature: emission in the solid state is assumed to occur from two luminescence centers with different excited-state lifetimes. This assumption leads to a conclusion that the *A* factors, A_f and A_s, in eq 4 are proportional to the population of each luminescent center. The population ratios, γ_f and γ_s, of the emissive states responsible for the faster and slower decays are formulated as

$$\gamma_f = A_f/(A_s + A_f) \text{ and } \gamma_s = A_s/(A_s + A_f) \quad (5)$$

The values γ_f and γ_s are found to be 0.66 and 0.34 for sample 1 and 0.15 and 0.85 for sample 5, from which it can be seen that the population of the slower decay increases dramatically in sample 5. From eq 4, ratios R_f and R_s of the emission yield for the faster and slower decay components to those of the total emission yield are formulated as

$$R_f = A_f\tau_f/(A_f\tau_f + A_s\tau_s) \text{ and } R_s = A_s\tau_s/(A_f\tau_f + A_s\tau_s) \quad (6)$$

The values of R_f and R_s are obtained as 0.50 and 0.50 for sample 1 and 0.02 and 0.98 for sample 5. Similarly, the contribution of the slower decay component to the total emission yield is largely improved and becomes the dominating component.

Decreased Nonradiative Rate Constant. The emission yield, Φ, is generally formulated as

$$\Phi = \Phi_E k_r \tau \quad (7)$$

$$1 \geq \Phi_E \geq \Phi \quad (8)$$

Here, Φ_E, k_r, and τ denote the quantum yield for the formation of the emissive state, the radiative rate constant of the emissive state, and the observed excited-state lifetime, respectively. Emission yields of the faster and slower components, Φ_f and Φ_s, are thus given by

$$\Phi_f = \Phi_T R_f = \Phi_E \gamma_f k_{r,f} \tau_f \text{ and } \Phi_s = \Phi_T R_s = \Phi_E \gamma_s k_{r,s} \tau_s \quad (9)$$

where Φ_T, $k_{r,f}$, $k_{r,s}$, τ_f, and τ_s denote the total emission yield, the faster decay radiative rate constant, the slower decay radiative rate constant, and the lifetime of the faster and slower decay components, respectively. Hereafter, it is assumed that $\Phi_E = 1.0$. With this assumption, the values of $k_{r,f}$ and $k_{r,s}$ are obtained as $4.1 \times 10^4\ S^{-1}$ and $4.1 \times 10^4\ S^{-1}$ for sample 1 and $1.1 \times 10^5\ S^{-1}$ and $1.9 \times 10^5\ S^{-1}$ for sample 5. It is clear that value of $k_{r,f}$ is quite similar to that of $k_{r,s}$ in samples 1 and 5, confirming that the slower and faster components of the emission originate from the same electronic excited state in samples 1 and 5. Clearly, $k_{r,f}$ for sample 5 is ~2.7 times larger than that of sample 1, and $k_{r,s}$ of sample 5 is ~4.6 times larger than that of sample 1. Considering that the total emission yield of sample 5 is 6.0 times larger than that of sample 1, the difference in nonradiative decay processes between the two samples may be anther reason for the obvious emission yield improvement of sample 5.

The weighted-average lifetime, $\bar{\tau}$, is formulated as

$$\bar{\tau} = (A_f\tau_f^2 + A_s\tau_s^2)/(A_f\tau_f + A_s\tau_s) \quad (10)$$

The usual expression of the excited-state lifetime formula is given by

$$\bar{\tau}^{-1} = \bar{k}_r + \bar{k}_{nr} \quad (11)$$

Here, $\bar{k}_r$ and $\bar{k}_{nr}$ denote the average radiative rate constant and nonradiative rate constant, respectively. With the help of eq 10, $\bar{k}_r$ and $\bar{k}_{nr}$ are found to be $3.7 \times 10^4\ S^{-1}$ and $2.0 \times 10^5\ S^{-1}$ for sample 1 and $9.6 \times 10^4\ S^{-1}$ and $4.0 \times 10^3\ S^{-1}$ for sample 5. The $\bar{k}_r$ value of sample 5 is 2.6 times larger than that of sample 1, whereas $\bar{k}_{nr}$ of sample 5 is 50 times smaller than that of sample 1. Thus, it is concluded that the dramatically improved emission yield of sample 5 is mainly caused by the effective suppression of the nonradiative decay process.

Structure of PE-[Cu(phen)(POP)]BF_4. *Estimation of Structure.* Blaskie and McMillin first reported that the excited state of Cu(I) complexes typically prefers a tetragonally flattened geometry whereas the ground state usually adopts a more tetrahedral-like coordination geometry appropriate for a closed-shell ion. Aside from reducing the energy content, the geometry relaxation that occurs in the excited state facilitates relaxation back to the ground state. By now, many other studies have confirmed the mechanism. According to the above analyses, (1) the molecular structure of sample 5 is identical to that of sample 1; (2) the weak intermolecular interaction between [Cu(phen)(POP)]BF_4 molecules is responsible for the formation of the metastable state; (3) the formation of the metastable state can effectively suppress the geometry relaxation, and it can be inferred that π stacking of [Cu(phen)(POP)]BF_4 molecules, which has been reported and confirmed by McMillin and co-workers, should be the above-mentioned intermolecular weak interaction and should be responsible for the formation of the metastable state.[22]

Explanation of Photophysical Property Variations of PE-[Cu(phen)(POP)]BF_4. Figure 5 depicts the π stacking of [Cu(phen)(POP)]BF_4 molecules, from which it can be found that two [Cu(phen)(POP)]BF_4 molecules are bonded head to head (the phen moiety is defined as the head) as a result of the $\pi-\pi$ attraction between two phens' π surfaces. According to a previous report, the aromatic rings lie almost parallel to one another. The mean planes through these two aromatic rings show a dihedral angle of ~4 °, and the mean distance between the planes is 3.35 Å, which is approximately the optimal π-stacking distance between two parallel aromatic rings.[22,25] It is believed that this bonded dual-molecule structure is a rigid one to some extent, which leads to the effective suppression of nonradiative decay that occurs in the excited state. Similarly, energy lost in the excited state also decreases, leading to the above-mentioned large-scale emission blue shift. This result is similar to the previous report of Thummel and coworks.[25] Solid state S-[Cu(phen)(POP)]BF_4 has nearly identical photophysical properties to those in the literature measured using low-concentration doped films, indicating that molecules of solid-state S-[Cu(phen)(POP)]BF_4 do not take the bonded dual-molecule structure.[13,24]

The *n*-hexane that is added to the solution of [Cu(phen)(POP)]BF_4 should function as a medium that facilitates the formation of dual-molecule structure. It is known that the POP moiety is more likely to be solvated in *n*-hexane than the phen moiety as a result of the POP's hydrophobicity. Thus, in an *n*-hexane environment, molecules of [Cu(phen)(POP)]BF_4 are more likely to take the head-to-head arrangement, which facilitates the formation of dual-molecule structure. Quantum calculation reveals that the dipole moment (μ) of the [Cu(phen)(POP)]$^+$ moiety is as large as 4.94 D. Thus, the head-to-head arrangement needs additional energy to overcome the coulomb repulsion between two [Cu(phen)(POP)]$^+$ moieties, which explains why low temperature can suppress the transformation from S-[Cu(phen)(POP)]BF_4 to PE-[Cu(phen)(POP)]BF_4.

As we mentioned, sample 1 exhibits stronger absorption in the 430−510 nm region than does sample 5 because of the somehow decreased oscillator strength of the transitions. This can also

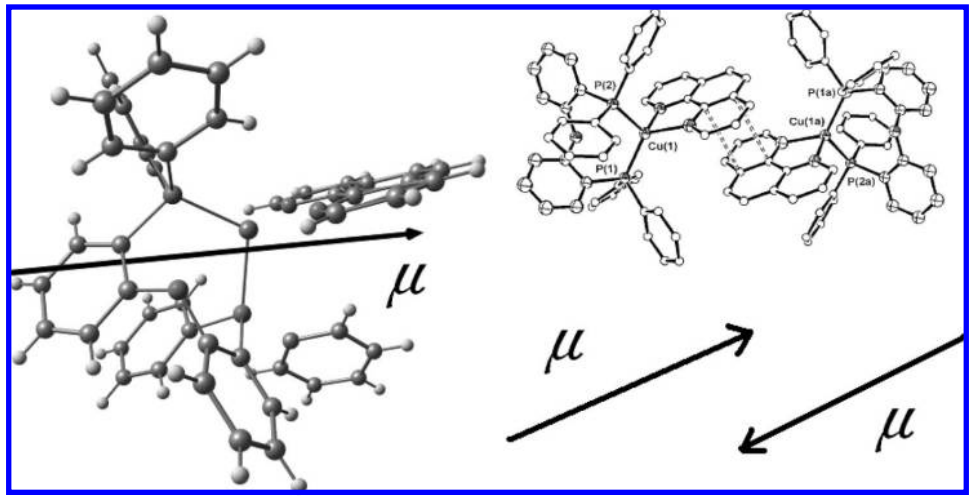

Figure 5. π stacking of [Cu(phen)(POP)]BF$_4$ and the dipole moment of [Cu(phen)(POP)]$^+$.

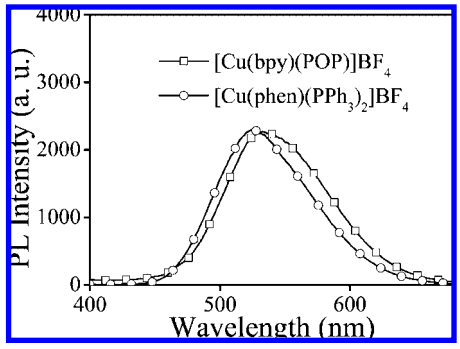

Figure 6. PL spectra of PE-[Cu(phen)(PPh$_3$)$_2$]BF$_4$ and PE-[Cu(bpy)-(POP)]BF$_4$ with λ_{ex} = 350 nm.

give an explanation of the dual-molecule structure as follows. The probability of a transition, σ, is given by

$$\sigma = \frac{8\pi^2}{3h^2}\langle\psi_i|\mu|\psi_j\rangle^2\rho(\nu_{if})t \qquad (12)$$

where $\rho(\nu_{if})$ denotes the radiation energy density of a transition with frequency of ν_{if}, t is the radiation time, $\langle\psi_i|\mu|\psi_j\rangle$ is called transition moment with an initial wave function of ψ_i and a final wave function of ψ_j, and μ is the dipole operator. From eq 12, it can be found that σ is proportional to the square of transition dipole moment. Because of the head-to-head molecular arrangement, the MLCT transition dipole moment of the dual-molecule structure may be decreased, leading to sample 5's weaker MLCT absorption.

Universality of π-Stacking Effect on Cu(I) Complexes. The structural and photophysical properties of [Cu(phen)(PPh$_3$)$_2$]BF$_4$ and [Cu(bpy)(POP)]BF$_4$ have also been reported, and we consult the photophysical properties of [Cu(phen)(PPh$_3$)$_2$]BF$_4$ and [Cu(bpy)(POP)]BF$_4$ after being processed by method B to confirm the universality of the π-stacking effect on Cu(I) complexes.[13,24] Figure 6 shows the PL spectra of PE-[Cu(phen)(PPh$_3$)$_2$]BF$_4$ and PE-[Cu(bpy)(POP)]BF$_4$ (λ_{ex} = 350 nm). Average excited-state lifetimes ($\bar{\tau}$),γ_f, γ_s, R_f, and R_s as well as their standard emission peak values are summarized in Table 1. It can be seen that samples processed using method B exhibit an obvious emission blue shift and excited-state lifetimes are longer than those of standard ones, which is similar to the case of PE-[Cu(phen)(POP)]BF$_4$. The trend that the contribution of the slower decay component to total emission yield is largely

Table 1. Photophysical Parameters of Cu(I) Complexes

	[Cu(phen)(PPh$_3$)$_2$]BF$_4$		[Cu(bpy)(POP)]BF$_4$	
compound	PE-	S-[a]	PE-	S-[b]
λ_{em} (nm)[c]	525	543	533	560
$\bar{\tau}$ (μs)[d]	9.6	8.1	4.3	1.2
γ_f	0.23	0.46	0.02	0.53
γ_s	0.77	0.54	0.98	0.47
R_f	0.05	0.12	0.08	0.19
R_s	0.95	0.88	0.92	0.81

[a] See ref 13. [b] See ref 24. [c] Emission peak wavelength with λ_{ex} = 350 ± 1 nm. [d] Experimental errors are ±5%.

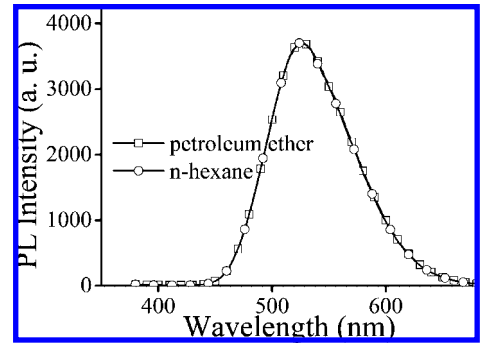

Figure 7. PL spectra of [Cu(phen)(POP)]BF$_4$ processed by *n*-hexane and petroleum ether with λ_{ex} = 350 nm.

improved and becomes the dominating component is also observed for PE-[Cu(phen)(PPh$_3$)$_2$]BF$_4$ and PE-[Cu(bpy)-(POP)]BF$_4$. Thus, it can be concluded that Cu(I) complexes with the structure of [Cu(N−N)(P−P)]$^+$ all undergo phosphorescence enhancement triggered by π stacking in the solid state if the diimine ligand can supply a π surface. The trends in emission blue shift and prolonged excited-state lifetime are consistent with the previous report about the π-stacking effect on Cu(I) complexes.[25]

Further Confirmation of the π-Stacking Effect on Cu(I) Complexes. Considering that PE-[Cu(phen)(POP)]BF$_4$ prepared in the suspension liquid of *n*-hexane and higher temperature can transform PE-[Cu(phen)(POP)]BF$_4$ back to S-[Cu(phen)-(POP)]BF$_4$, there is thus the possibility of the *n*-hexane molecule's effect on [Cu(phen)(POP)]BF$_4$, which leads to the phosphorescence enhancement, even though the probability is slim because PE-[Cu(phen)(POP)]BF$_4$ dried in vacuum at 30 °C retains its enhanced phosphorescence. Thus, we come to the following

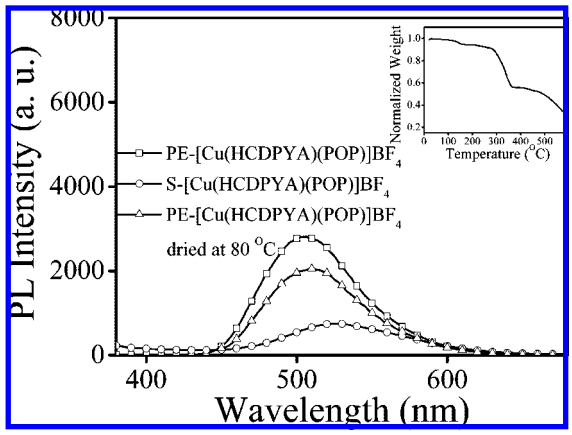

Figure 8. PL spectra of S-, PE-, and thermally processed PE-[Cu(HCDPYA)(POP)]BF_4. The inset shows the TGA of thermally processed PE-[Cu(HCDPYA)(POP)]BF_4.

experiments: (1) *n*-Hexane was replaced by petroleum ether during the transformation cycle. The PL spectrum of the resulting [Cu(phen)(POP)]BF_4 is identical to that of PE-[Cu(phen)-(POP)]BF_4 prepared using method B as shown in Figure 7. (2) A new diimine ligand, HCDYPA, was synthesized to further confirm the phosphorescence enhancement triggered by π stacking. According to the above analyses, the [Cu(phen)-(POP)]BF_4 molecule takes the head-to-head dual-molecule structure, and π-attraction in the dual-molecule structure is so weak that it can be broken by high temperature. The hydrogen bond between two HCDPYA molecules may provide an additional attraction in the dual-molecule structure so that the dual-molecule structure may be stable enough to experience high temperature. In addition, π stacking should be more stable because of the more rigid π surface of HCDPYA compared with that of bpy. Phosphorescence-enhanced [Cu(HCDPYA)(POP)]BF_4 was processed using method B and dried at 80 °C in vacuum for 8 h to eliminate *n*-hexane (bp 68.7 °C). The inset of Figure 8 demonstrates the thermogravimetric analysis (TGA) of PE-[Cu(HCDPYA)(POP)]BF_4, from which it can be seen that no *n*-hexane exists in the sample. As shown in Figure 8, the PL spectrum of standard [Cu(HCDPYA)(POP)]BF_4 has a peak at 526 nm, and the corresponding values of phosphorescence-enhanced and thermally processed PE-[Cu(HCDPYA)(POP)]-BF_4 are 505 and 508 nm, respectively, indicating that the dual-molecule structure of PE-[Cu(HCDPYA)(POP)]BF_4 is stable enough to experience high temperature because of the enhanced π attraction supplied by HCDPYA. Thus, the possibility of the *n*-hexane molecule's effect on Cu(I) complexes is eliminated, which further confirms that phosphorescence enhancement is caused by nonradiative process suppression due to π-stacking in Cu(I) complexes.

Conclusions

The previously well studied and reported [Cu(phen)(POP)]-BF_4 exhibits new features: the phosphorescence is largely enhanced after being processed by *n*-hexane or petroleum ether, including a large-scale emission blue shift, a dramatically improved emission yield, and a longer excited-state lifetime. Systematic studies reveal that the main cause of this phenomenon is nonradiative process suppression triggered by the π stacking between [Cu(N−N)(P−P)]BF_4 molecules. This phenomenon exists widely in [Cu(N−N)(P−P)]BF_4 complexes that have π surfaces in their diimine ligands.

Acknowledgment. We are grateful for financial support from the One Hundred Talents Project of the Chinese Academy of Sciences and the National Natural Science Foundation of China (grant no. 50872130).

Supporting Information Available: X-ray diffraction patterns of samples 1 and 5. This material is available free of charge via the Internet at http://pubs.acs.org.

LA803822S